Table 3 Behavioral and affective reactions

	Placebo median (IQR)	Modafinil median (IQR)
Reaction time (ms)		
+¥0	235.59 (219.67–252.48)	225.75 (215.05–252.18)
+¥20	226.55 (215.10–232.59)	218.31 (211.07–238.77)
+¥100	223.57 (216.11–231.13)	222.50 (214.82–235.24)
+¥500	224.22 (211.35–229.35)	217.05 (199.51–238.18)
−¥0	232.57 (222.29–247.49)	227.28 (214.05–241.51)
−¥20	226.60 (212.60–240.38)	230.98 (218.29–242.11)
−¥100	231.88 (209.90–239.70)	225.46 (216.45–243.59)
−¥500	219.00 (215.74–228.98)	228.25 (211.79–240.42)
VAS for effort		
+¥0	7.15 (5.38–8.48)	7.20 (4.78–9.30)
+¥20	7.55 (6.45–9.40)	7.80 (6.55–9.75)
+¥100	9.00 (7.58–10.00)	9.25 (7.98–9.90)
+¥500*	9.75 (9.10–10.00)	10.00 (9.58–10.00)
−¥0	6.45 (4.98–9.03)	7.30 (4.88–9.45)
−¥20	8.55 (6.73–9.50)	8.30 (6.28–9.93)
−¥100	9.35 (7.95–10.00)	9.25 (7.93–9.93)
−¥500*	9.80 (9.55–10.00)	10.00 (9.80–10.00)

IQR interquartile range, *VAS* visual analogue scale

*$p < 0.05$ between placebo and modafinil treatments

conditions in all brain areas including the NAc ($p < 0.001$ uncorrected).

NAc ROI analysis of gain and loss anticipations in the MID task under the placebo and modafinil conditions

We further focused on the NAc activity as an *a priori* ROI for gain and loss anticipations under the modafinil condition during the MID task. We constructed bilateral NAc ROIs with default settings of the right and left NAc in the WFU PickAtlas.

Activations under the placebo condition

The contrast of gain anticipation revealed that the BOLD signal was increased in the left NAc, while the contrast of loss anticipation showed no activation in NAc ($p < 0.05$ FWE-corrected; Fig. 2).

Activations under the modafinil condition

The contrast of gain and loss anticipations revealed that the BOLD signals were increased in the bilateral and left NAc, respectively ($p < 0.05$ FWE-corrected; Fig. 2).

Direct dose-wise differences

Group-level analyses revealed that modafinil did not show a significant increase in BOLD signal in the NAc during gain and loss anticipations as compared with the placebo ($p < 0.05$ FWE-corrected for NAc ROI). We next examined the percent changes in BOLD signal of individual cues. In the gain anticipation, the modafinil condition showed higher BOLD signal change at the +¥500 gain cue than the placebo condition ($p = 0.048$; Fig. 3). In loss anticipation, however, there were no significant differences for any of the incentive cues between the placebo and modafinil conditions (Fig. 3). There were no significant correlations between percent signal change and VAS for effort in the placebo ($p = 0.862$ for + ¥500, $p = 0.836$ for −¥500) or in the modafinil condition ($p = 0.734$ for +¥500, $p = 0.258$ for −¥500).

Discussion

In this study, BOLD signals were increased in several brain regions including the NAc during gain and loss anticipations. These results clearly show that the present fMRI study with the MID task could efficiently depict the functional role of the NAc in the reward system, consistent with previous results (Carter et al. 2009; Saji et al. 2013). Although the overall effects of modafinil on BOLD signals in the NAc during the anticipations were not significant as compared with those of the placebo, modafinil caused larger BOLD signal change than the placebo during the gain anticipation for the +¥500 cue. Previous pharmacological fMRI studies have shown that dopamine-releasing agents increase the BOLD signal in the NAc in humans (Knutson and Gibbs 2007; Oei et al. 2012). L-dopa, a dopamine precursor, is effective in increasing BOLD activity during the reward task in elderly subjects (Chowdhury et al. 2013). In addition, an fMRI study combined with PET measures also demonstrated that the BOLD response to reward anticipation in the NAc correlates positively with dopamine release in the NAc during a reward task in humans (Buckholtz et al. 2010; Schott et al. 2008). Modafinil at therapeutic doses binds to the dopamine transporters (Madras et al. 2006; Zolkowska et al. 2009) and inhibits dopamine reuptake, resulting in significant dopamine release in the NAc (Volkow et al. 2009). Collectively, the present study provides the first evidence that modafinil modulates positive reward processing (gain anticipation), possibly by increasing extracellular dopamine in the NAc through dopamine transporter inhibition.

Interestingly, modafinil showed larger BOLD signal change compared with the placebo during the highest gain anticipation. On the other hand, Knutson et al. (Knutson et al. 2004) reported that amphetamine elicits reduced peak activation at the highest gain level and increased peak activation at

Table 4 Activation by gain and loss anticipation under placebo and modafinil conditions

Contrast	Region	BA		Talairach coordinates			
				X	y	z	t value
Gain anticipation							
Placebo	Nucleus accumbens		L	−16	9	−11	3.57*
	Insula	13	L	−46	6	2	5.26
		13	R	40	2	7	4.67
	Medial frontal gyrus	6	L	−8	0	48	6.98
			R	2	4	50	6.80
	Inferior frontal gyrus	44	R	63	7	16	5.52
	Thalamus		L	−12	−15	10	6.93
			R	16	−15	12	6.90
	Precentral gyrus	6	L	−24	−23	49	6.86
		6	R	26	−15	56	4.51
	Posterior cingulate	23	R	6	−28	24	7.00
	Postcentral gyrus	2	R	44	−23	44	4.19
	Paracentral lobule	5	R	6	−35	48	3.75
	Precuneus	7	R	20	−55	34	5.22
	Middle occipital gyrus	18	L	−28	−89	1	12.25
			R	34	−85	3	9.44
	Cerebellum		R	22	−41	−33	4.19
Modafinil	Nucleus accumbens		L	−16	9	−11	5.34
			R	14	11	−7	4.10
	Middle frontal gyrus	6	L	−16	−11	58	9.14
	Precentral gyrus	6	L	−46	−2	41	8.70
	Cuneus	18	L	−26	−93	−2	8.68
Loss anticipation							
Placebo	Putamen		L	−18	4	0	4.72
	Insula	13	L	−28	−26	18	8.37
	Cingulate gyrus	24	L	−14	9	29	4.89
	Precentral gyrus	6	L	−36	−6	33	7.88
	Precuneus	7	R	12	−56	43	4.66
Modafinil	Putamen		L	−22	−7	6	4.18
			R	28	−16	−4	6.28
	Thalamus		R	4	−13	3	5.64
	Insula	13	L	−40	12	−2	4.48
		13	R	36	6	0	6.59
	Superior frontal gyrus	10	R	36	55	16	3.92
	Middle frontal gyrus	46	R	42	49	9	5.09
	Medial frontal gyrus	6	L	−10	−1	57	7.58
	Inferior frontal gyrus	46	R	48	41	7	5.49
	Precentral gyrus	4	R	46	−9	50	7.33
	Superior temporal gyrus	22	L	−53	8	0	4.95
		22	R	57	8	1	7.26
	Inferior occipital gyrus	18	L	−34	−88	−6	6.41
	Inferior parietal lobule	40	R	55	−42	24	7.27
	Cuneus	17	L	−6	−71	11	4.53
			R	2	−73	13	4.35
	Cerebellum		R	4	−49	−16	7.28

All other results $p < 0.001$ uncorrected

BA Brodmann area, *L* left, *R* right

*$p < 0.05$ FWE-corrected for nucleus accumbens

Fig. 2 Neural responses to gain anticipation in the bilateral nucleus accumbens. **a** Brain activation in the bilateral nucleus accumbens during gain anticipation under placebo and **b** modafinil conditions. Familywise error-corrected $p<0.05$. *Color bar* indicates t statistics
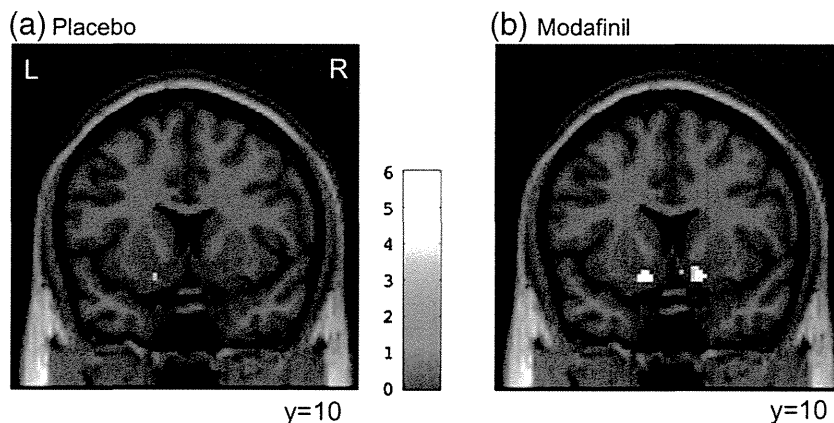
the middle loss level, resulting in equalization of the NAc activity levels. They speculated that this result was due to enhancement of tonic dopaminergic activation over phasic activation by amphetamine (Knutson et al. 2004). Mesolimbic dopamine neurons transmit dopamine signals in tonic and phasic mode, and phasic dopamine responses are triggered by many types of rewards and reward-related sensory cues (Bromberg-Martin et al. 2010). Previous animal studies have shown that the extracellular level of dopamine is largely established by phasic dopamine release (Owesson-White et al. 2012) and that dopamine transporter inhibition increases extracellular dopamine levels, changing both frequency and size of dopamine transients in the NAc (Heien et al. 2005; Owesson-White et al. 2012; Robinson and Wightman 2004). Thus, modafinil appears to bind to and inhibit dopamine transporters (Minzenberg and Carter 2008), resulting in changes in both frequency and size of dopamine transients (Heien et al. 2005; Owesson-White et al. 2012; Robinson and Wightman 2004), whereas amphetamine raises extracellular dopamine levels by inducing stimulation-independent dopamine efflux via reverse transport through the DA transporter and decreases stimulation-dependent

vesicular dopamine release (Schmitz et al. 2001; Sulzer et al. 2005).

The reason why modafinil showed significantly larger BOLD signal change compared with the placebo at the highest gain cue, but minimal change at other cues, remains unknown. It is intriguing that tyrosine/phenylalanine depletion, which is expected to result in reduction of dopamine synthesis, causes reduction in percent signal change in the BOLD signal in the NAc compared with a control condition during only the higher gain anticipation with a similar reward task (Bjork et al. 2013). In a previous study with reward task using low incentive, there were no significant effects of modafinil on low incentive reward in patients with a first episode of psychosis (Scoriels et al. 2011).

The brain reward circuitry has been reported to be dysregulated in patients with several psychiatric disorders, including substance use disorders, schizophrenia, depression, and pathological gambling (Chau et al. 2004; Reuter et al. 2005; Russo and Nestler 2013). Several drugs have been proposed as candidates to treat such dysfunction in the reward circuitry (Forray and Sofuoglu 2012; Green et al. 2008; Leung and Cottler 2009). For instance, bupropion, which inhibits
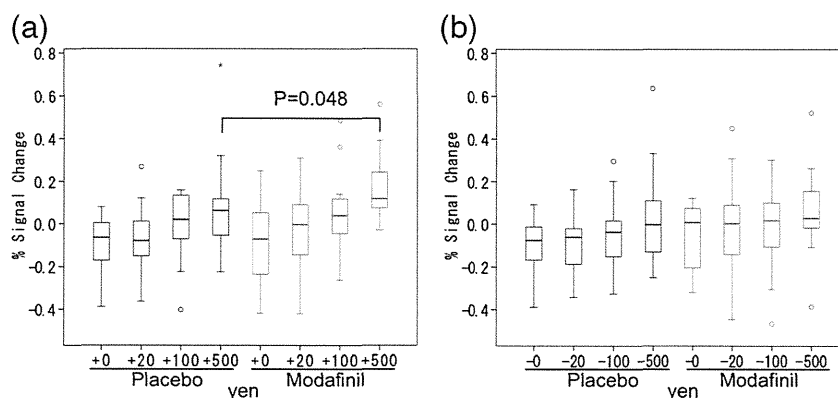

Fig. 3 Percent signal changes in the left nucleus accumbens during **a** gain and **b** loss anticipation. *Lower and upper hinges of boxes* denote 25th and 75th percentiles, respectively. Median (50th percentile) of each distribution is indicated by *solid line. Whiskers on either side* extend to either the most extreme data point or median±1.5 times the interquartile range. The *circles* are outliers meaning data points outside interquartile range

dopamine and norepinephrine reuptake, reduces use among light methamphetamine users (Forray and Sofuoglu 2012). In patients with schizophrenia and major depression, anhedonia driven by loss of reward function is a serious symptom requiring treatment (Choi et al. 2013; Der-Avakian and Markou 2012). Modafinil at a therapeutic dose enhanced larger gain anticipation in our study, and it might augment pleasurable effects of reward. Therefore, the present results could help to discover appropriate treatments of anhedonia and facilitate our understanding of the brain reward circuitry.

Limitations of the study

In this study we examined the effects of single-dose modafinil on the reward system. However, to treat patients with schizophrenia and major depression, modafinil needs to be chronically administered. Further, anhedonia scales were not assessed. Therefore, we need to further clarify the effectiveness of chronic modafinil administration in these patients using appropriate clinical measures.

In addition, we focused on the dopaminergic system to discuss modafinil effects in the present study. However, the involvement of other neurotransmitter systems in modafinil effects will remain to be further analyzed in the NAc because modafinil exerts its effects on a number of neurotransmitter systems other than catecholamines, including glutamate, serotonin, orexin, and histamine.

References

Andersen ML, Kessler E, Murnane KS, McClung JC, Tufik S, Howell LL (2010) Dopamine transporter-related effects of modafinil in rhesus monkeys. Psychopharmacology (Berl) 210:439–448. doi:10.1007/s00213-010-1839-2

Beck AT, Steer RA, Brown GK (1996) Manual for the Beck Depression Inventory (2nd ed.) Pearson, Texas

Bjork JM, Grant SJ, Chen G, Hommer DW (2013) Dietary tyrosine/phenylalanine depletion effects on behavioral and brain signatures of human motivational processing. Neuropsychopharmacology. doi:10.1038/npp.2013.232

Bobo WV, Woodward ND, Sim MY, Jayathilake K, Meltzer HY (2011) The effect of adjunctive armodafinil on cognitive performance and psychopathology in antipsychotic-treated patients with schizophrenia/schizoaffective disorder: a randomized, double-blind, placebo-controlled trial. Schizophr Res 130:106–113. doi:10.1016/j.schres.2011.05.015

Bromberg-Martin ES, Matsumoto M, Hikosaka O (2010) Dopamine in motivational control: rewarding, aversive, and alerting. Neuron 68:815–834. doi:10.1016/j.neuron.2010.11.022

Buckholtz JW, Treadway MT, Cowan RL, Woodward ND, Benning SD, Li R, Ansari MS, Baldwin RM, Schwartzman AN, Shelby ES, Smith CE, Cole D, Kessler RM, Zald DH (2010) Mesolimbic dopamine reward system hypersensitivity in individuals with psychopathic traits. Nat Neurosci 13:419–421. doi:10.1038/nn.2510

Carter RM, Macinnes JJ, Huettel SA, Adcock RA (2009) Activation in the VTA and nucleus accumbens increases in anticipation of both gains and losses. Front Behav Neurosci 3:21. doi:10.3389/neuro.08.021.2009

Chau DT, Roth RM, Green AI (2004) The neural circuitry of reward and its relevance to psychiatric disorders. Curr Psychiatry Rep 6:391–399. doi:10.1007/s11920-004-0026-8

Choi SH, Lee H, Ku J, Yoon KJ, Kim JJ (2013) Neural basis of anhedonia as a failure to predict pleasantness in schizophrenia. World J Biol Psychiatry. doi:10.3109/15622975.2013.81921

Chowdhury R, Guitart-Masip M, Lambert C, Dayan P, Huys Q, Düzel E, Dolan RJ (2013) Dopamine restores reward prediction errors in old age. Nat Neurosci 16:648–653. doi:10.1038/nn.3364

Der-Avakian A, Markou A (2012) The neurobiology of anhedonia and other reward-related deficits. Trends Neurosci 35:68–77. doi:10.1016/j.tins.2011.11.005

Forray A, Sofuoglu M (2012) Future Pharmacological Treatments for Substance Use Disorders. Br J Clin Pharmacol. doi:10.1111/j.1365-2125.2012.04474.x

Gold LH, Balster RL (1996) Evaluation of the cocaine-like discriminative stimulus effects and reinforcing effects of modafinil. Psychopharmacology (Berl) 126:286–292. doi:10.1007/BF02247379

Green AI, Noordsy DL, Brunette MF, O'Keefe C (2008) Substance abuse and schizophrenia: pharmacotherapeutic intervention. J Subst Abuse Treat 34:61–71. doi:10.1016/j.jsat.2007.01.008

Haber SN, Knutson B (2010) The reward circuit: linking primate anatomy and human imaging. Neuropsychopharmacology 35:4–26. doi:10.1038/npp.2009.129

Heien MLAV, Khan AS, Ariansen JL, Cheer JF, Phillips PEM, Wassum KM, Wightman RM (2005) Real-time measurement of dopamine fluctuations after cocaine in the brain of behaving rats. Proc Natl Acad Sci U S A 102:10023–10028. doi:10.1073/pnas.0504657102

Hidano T, Fukuhara M, Iwawaki M, Soga S, Spielberger CD (2000) State-Trait Anxiety Inventory – form JYZ. Jitsumukyoiku Shuppan, Tokyo

Inada T (2010) Evaluation training seat of structured interview guide for Hamilton Anxiety Scale ver1.1. The Japanese Society of Psychiatric Rating Scales, Tokyo

Johns MW (1991) A new method for measuring daytime sleepiness: the Epworth sleepiness scale. Sleep 14:540–545

Knutson B, Adams CM, Fong GW, Hommer D (2001) Anticipation of increasing monetary reward selectively recruits nucleus accumbens. J Neurosci 21:RC159

Knutson B, Bhanji JP, Cooney RE, Atlas LY, Gotlib IH (2008) Neural responses to monetary incentives in major depression. Biol Psychiatry 63:686–692. doi:10.1016/j.biopsych.2007.07.023

Knutson B, Bjork JM, Fong GW, Hommer D, Mattay VS, Weinberger DR (2004) Amphetamine modulates human incentive processing. Neuron 43:261–269. doi:10.1016/j.neuron.2004.06.030

Knutson B, Greer SM (2008) Anticipatory affect: neural correlates and consequences for choice. Philos Trans R Soc Lond B BiolSci 363:3771–3786. doi:10.1098/rstb.2008.0155

Knutson B, Gibbs SE (2007) Linking nucleus accumbens dopamine and blood oxygenation. Psychopharmacology 191:813–822. doi:10.1007/s00213-006-0686-7

Kojima M, Furukawa TA (2003) Japanese Manual of the Beck Depression Inventory (2nd ed.). Nihon Bunka Kagakusha, Tokyo

Leung KS, Cottler LB (2009) Treatment of pathological gambling. Curr Opin Psychiatry 22:69–74. doi:10.1097/YCO.0b013e32831575d9

Lynch G, Palmer LC, Gall CM (2011) The likelihood of cognitive enhancement. Pharmacol Biochem Behav 99:116–129. doi:10.1016/j.pbb.2010.12.024

Madras BK, Xie Z, Lin Z, Jassen A, Panas H, Lynch L, Johnson R, Livni E, Spencer TJ, Bonab AA, Miller GM, Fischman AJ (2006) Modafinil occupies dopamine and norepinephrine transporters in vivo and modulates the transporters and trace amine activity in vitro. J Pharmacol Exp Ther 319:561–569. doi:10.1124/jpet.106.106583

McNair DM, Lorr M, Droppleman LF (1992) Profile of Mood States. Educational and Industrial Testing Service, San Diego

Minzenberg MJ, Carter CS (2008) Modafinil: a review of neurochemical actions and effects on cognition. Neuropsychopharmacology 33:1477–1502. doi:10.1038/sj.npp.1301534

Minzenberg MJ, Yoon JH, Carter CS (2011) Modafinil modulation of the default mode network. Psychopharmacology (Berl) 215:23–31. doi:10.1007/s00213-010-2111-5

Müller U, Steffenhagen N, Regenthal R, Bublak P (2004) Effects of modafinil on working memory processes in humans. Psychopharmacology (Berl) 177:161–169. doi:10.1007/s00213-004-1926-3

Nakane Y, Williams JBW (2003) A structured interview guide for the Hamilton Depressive Rating Scale Japanese version. Rinsho Seishin Yakuri 6:1353–1368

Nguyen TL, Tian YH, You IJ, Lee SY, Jang CG (2011) Modafinil-induced conditioned place preference via dopaminergic system in mice. Synapse 65:733–741. doi:10.1002/syn.20892

Norris H (1971) The action of sedatives on brain stem oculomotor systems in man. Neuropharmacology 10:181–191. doi:10.1016/0028-3908(71)90039-6

Oei NY, Rombouts SA, Soeter RP, van Gerven JM, Both S (2012) Dopamine modulates reward system activity during subconscious processing of sexual stimuli. Neuropsychopharmacology 37:1729–1737. doi:10.1038/npp.2012.19

Oldfield RC (1971) The assessment and analysis of handedness: the Edinburgh inventory. Neuropsychologia 9:97–113. doi:10.1016/0028-3932(71)90067-4

Owesson-White CA, Roitman MF, Sombers LA, Belle AM, Keithley RB, Peele JL, Carelli RM, Wightman RM (2012) Sources contributing to the average extracellular concentration of dopamine in the nucleus accumbens. J Neurochem 121:252–262. doi:10.1111/j.1471-4159.2012.07677.x

Peters J, Büchel C (2011) The neural mechanism of inter-temporal decision-making: understanding variability. Trends Cogn Sci 15:227–239. doi:10.1016/j.tics.2011.03.002

Piérard C, Liscia P, Philippin JN, Mons N, Lafon T, Chauveau F, Van Beers P, Drouet I, Serra A, Jouanin JC, Béracochéa D (2007) Modafinil restores memory performance and neural activity impaired by sleep deprivation in mice. Pharmacol Biochem Behav 88:55–63. doi:10.1016/j.pbb.2007.07.006

Qu WM, Huang ZL, Xu XH, Matsumoto N, Urade Y (2008) Dopaminergic D_1 and D_2 receptors are essential for the arousal effect of modafinil. J Neurosci 28:8462–8469. doi:10.1523/JNEUROSCI.1819-08.2008

Randall DC, Viswanath A, Bharania P, Elsabagh SM, Hartley DE, Shneerson JM, File SE (2005) Does modafinil enhance cognitive performance in young volunteers who are not sleep-deprived? J Clin Psychopharmacol 25:175–179. doi:10.1097/01.jcp.0000155816.21467.25

Reuter J, Raedler T, Rose M, Hand I, Gläscher J, Büchel C (2005) Pathological gambling is linked to reduced activation of the mesolimbic reward system. Nat Neurosci 8:147–148. doi:10.1038/nn1378

Robertson P Jr, Hellriegel ET (2003) Clinical pharmacokinetic profile of modafinil. Clin Pharmacokinet 42:123–137. doi:10.2165/00003088-200342020-00002

Robinson DL, Wightman RM (2004) Nomifensine amplifies subsecond dopamine signals in the ventral striatum of freely-moving rats. J Neurochem 90:894–903. doi:10.1111/j.1471-4159.2004.02559.x

Russo SJ, Nestler EJ (2013) The brain reward circuitry in mood disorders. Nat Rev Neurosci 14:609–625. doi:10.1038/nrn3381

Saji K, Ikeda Y, Kim W, Shingai Y, Tateno A, Takahashi H, Okubo Y, Fukayama H, Suzuki H (2013) Acute NK_1 receptor antagonist administration affects reward incentive anticipation processing in healthy volunteers. Int J Neuropsychopharmacol 16:1461–1471. doi:10.1017/S1461145712001678

Schmitz Y, Lee CJ, Schmauss C, Gonon F, Sulzer D (2001) Amphetamine distorts stimulation-dependent dopamine overflow: effects on D2 autoreceptors, transporters, and synaptic vesicle stores. J Neurosci 21:5916–5924

Schott BH, Minuzzi L, Krebs RM, Elmenhorst D, Lang M, Winz OH, Seidenbecher CI, Coenen HH, Heinze HJ, Zilles K, Düzel E, Bauer A (2008) Mesolimbic functional magnetic resonance imaging activations during reward anticipation correlate with reward-related ventral striatal dopamine release. J Neurosci 28:14311–14319. doi:10.1523/JNEUROSCI.2058-08.2008

Schultz W (1997) Dopamine neurons and their role in reward mechanisms. Curr Opin Neurobiol 7:191–197. doi:10.1016/S0959-4388(97)80007-4

Scoriels L, Barnett JH, Murray GK, Cherukuru S, Fielding M, Cheng F, Lennox BR, Sahakian BJ, Jones PB (2011) Effects of modafinil on emotional processing in first episode psychosis. Biol Psychiatry 69:457–464. doi:10.1016/j.biopsych.2010.09.043

Scoriels L, Jones PB, Sahakian BJ (2013) Modafinil effects on cognition and emotion in schizophrenia and its neurochemical modulation in the brain. Neuropharmacology 64:168–184. doi:10.1016/j.neuropharm.2012.07.011

Shear MK, Vander Bilt J, Rucci P, Endicott J, Lydiard B, Otto MW, Pollack MH, Chandler L, Williams J, Ali A, Frank DM (2001) Reliability and validity of a structured interview guide for the Hamilton Anxiety Rating Scale (SIGH-A). Depress Anxiety 13:166–178. doi:10.1002/da.1033

Stoy M, Schlagenhauf F, Schlochtermeier L, Wrase J, Knutson B, Lehmkuhl U, Huss M, Heinz A, Ströhle A (2011) Reward processing in male adults with childhood ADHD–a comparison between drug-naïve and methylphenidate-treated subjects. Psychopharmacology 215:467–481. doi:10.1007/s00213-011-2166-y

Sulzer D, Sonders MS, Poulsen NW, Galli A (2005) Mechanisms of neurotransmitter release by amphetamines: a review. Prog Neurobiol 75:406–433. doi:10.1016/j.pneurobio.2005.04.003

Takegami M, Suzukamo Y, Wakita T, Noguchi H, Chin K, Kadotani H, Inoue Y, Oka Y, Nakamura T, Green J, Johns MW, Fukuhara S (2009) Development of a Japanese version of the Epworth Sleepiness Scale (JESS) based on item response theory. Sleep Med 10:556–565. doi:10.1016/j.sleep.2008.04.015

Talairach J, Tournoux P (1988) Co-planar Stereotaxic Atlas of the Human Brain: 3-Dimensional Proportional System—An Approach to Cerebral Imaging. Thieme Medical Publishers, New York

Turner DC, Clark L, Pomarol-Clotet E, McKenna P, Robbins TW, Sahakian BJ (2004) Modafinil improves cognition and attentional set shifting in patients with chronic schizophrenia. Neuropsychopharmacology 29:1363–1373. doi:10.1038/sj.npp.1300457

Volkow ND, Fowler JS, Logan J, Alexoff D, Zhu W, Telang F, Wang GJ, Jayne M, Hooker JM, Wong C, Hubbard B, Carter P, Warner D, King P, Shea C, Xu Y, Muench L, Apelskog-Torres K (2009) Effects of modafinil on dopamine and dopamine transporters in the male human brain: clinical implications. JAMA 301:1148–1154. doi:10.1001/jama.2009.351

Williams J, Link M, Rosenthal N, Terman M (1988) Structured Interview Guide for the Hamilton Rating Scale – Seasonal Affective Disorder Version (SIGH-SAD). New York State Psychiatric Institute, New York

Wisor JP, Nishino S, Sora I, Uhl GH, Mignot E, Edgar DM (2001) Dopaminergic role in stimulant-induced wakefulness. J Neurosci 21:1787–1794

Yacubian J, Gläscher J, Schroeder K, Sommer T, Braus DF, Büchel C (2006) Dissociable systems for gain- and loss-related value predictions and errors of prediction in the human brain. J Neurosci 26:9530–9537. doi:10.1523/JNEUROSCI.2915-06.2006

Yokoyama K, Araki S, Kawakami N, Takeshita T (1990) Production of the Japanese edition of profile of mood states (POMS): assessment of reliability and validity. Nippon Koshu Eisei Zasshi 37:913–918

Zolkowska D, Jain R, Rothman RB, Partilla JS, Roth BL, Setola V, Prisinzano TE, Baumann MH (2009) Evidence for the involvement of dopamine transporters in behavioral stimulant effects of modafinil. J Pharmacol Exp Ther 329:738–746. doi:10.1124/jpet.108.146142

ARTICLE

Norepinephrine transporter occupancy by nortriptyline in patients with depression: a positron emission tomography study with (S,S)-[18F]FMeNER-D2

Harumasa Takano[1], Ryosuke Arakawa[1], Tsuyoshi Nogami[1], Masayuki Suzuki[1],
Tomohisa Nagashima[1], Hironobu Fujiwara[1], Yasuyuki Kimura[1], Fumitoshi Kodaka[1],
Keisuke Takahata[1], Hitoshi Shimada[1], Yoshitaka Murakami[2], Amane Tateno[3],
Makiko Yamada[1], Hiroshi Ito[4], Kazunori Kawamura[5], Ming-Rong Zhang[5],
Hidehiko Takahashi[1], Motoichiro Kato[6], Yoshiro Okubo[3] and Tetsuya Suhara[1]

[1] *Clinical Neuroimaging Team, Molecular Neuroimaging Program, Molecular Imaging Center, National Institute of Radiological Sciences, Chiba, Japan*
[2] *Department of Medical Statistics, Shiga University of Medical Science, Shiga, Japan*
[3] *Department of Neuropsychiatry, Nippon Medical School, Tokyo, Japan*
[4] *Biophysics Program, Molecular Imaging Center, National Institute of Radiological Sciences, Chiba, Japan*
[5] *Molecular Probe Program, Molecular Imaging Center, National Institute of Radiological Sciences, Chiba, Japan*
[6] *Department of Neuropsychiatry, Keio University School of Medicine, Tokyo, Japan*

Abstract

Norepinephrine transporter (NET) plays important roles in the treatment of various neuropsychiatric disorders, such as depression and attention deficit hyperactivity disorder (ADHD). Nortriptyline is a NET-selective tricyclic antidepressant (TCAs) that has been widely used for the treatment of depression. Previous positron emission tomography (PET) studies have reported over 80% serotonin transporter occupancy with clinical doses of selective serotonin reuptake inhibitors (SSRIs), but there has been no report of NET occupancy in patients treated with relatively NET-selective antidepressants. In the present study, we used PET and (S,S)-[18F]FMeNER-D2 to investigate NET occupancies in the thalamus in 10 patients with major depressive disorder taking various doses of nortriptyline, who were considered to be responders to the treatment. Reference data for the calculation of occupancy were derived from age-matched healthy controls. The result showed approximately 50–70% NET occupancies in the brain as a result of the administration of 75–200 mg/d of nortriptyline. The estimated effective dose (ED_{50}) and concentration (EC_{50}) required to induce 50% occupancy was 65.9 mg/d and 79.8 ng/ml, respectively. Furthermore, as the minimum therapeutic level of plasma nortriptyline for the treatment of depression has been reported to be 70 ng/ml, our data indicate that this plasma nortriptyline concentration corresponds to approximately 50% NET occupancy measured with PET, suggesting that more than 50% of central NET occupancy would be appropriate for the nortriptyline treatment of patients with depression.

Introduction

Norepinephrine pathways in the brain play important roles in the regulation of cognitive functions such as attention, memory, mood, motivation, and vigilance. Norepinephrine transporter (NET) serves as one of the main targets of the treatment of various neuropsychiatric

disorders, such as depression and attention deficit hyperactivity disorder (ADHD) (Nestler et al., 2008). Although depression consists of various symptoms, and is considered to be a heterogeneous disease (Harald and Gordon, 2012), some symptoms such as psychomotor-slowing and decreased concentration are reportedly related to the norepinephrine system. Antidepressants acting on NET play critical roles in the treatment of depression, particularly in patients who present with significant levels of these symptoms (Frazer, 2000; Brunello et al., 2002; Uher et al., 2009; Dell'Osso et al., 2011; Kasper et al., 2011).

Nortriptyline is a tricyclic antidepressant (TCA) that has been widely used for the treatment of depression.

Address for correspondence: Tetsuya Suhara, Clinical Neuroimaging Team, Molecular Neuroimaging Program, Molecular Imaging Center, National Institute of Radiological Sciences, 4-9-1 Anagawa, Inage-ku, Chiba 263-8555, Japan.
Tel.: (+81) 43-206-3194 *Fax:* (+81) 43-253-0396
Email: suhara@nirs.go.jp

In particular, nortriptyline is regarded as a relatively NET-selective antidepressant because its binding affinity for NET is much higher than that for the other mono-amine transporters such as serotonin transporter (5-hydroxytryptamine transporter: 5-HTT) and dopamine transporter (Owens et al., 1997; Frazer, 2000, 2001; Vaishnavi et al., 2004; Gillman, 2007). Furthermore, it has been reported that there is a minimum effective level in the plasma concentration of nortriptyline in terms of clinical response, and also a maximum plasma concentration owing to a high incidence of side effects, although this may not necessarily be applicable to all patients (Baumann et al., 2004, 2005; Hiemke et al., 2011).

Recent advancements of suitable positron emission tomography (PET) radioligands for NET such as (S,S)-[^{18}F]FMeNER-D$_2$ and [^{11}C]MRB have made it possible to evaluate *in vivo* NET occupancy in the brain by psychotropic drugs. In nonhuman primates, atomoxetine, a selective NET inhibitor used for the treatment of ADHD, showed dose-dependent occupancies for NET using [^{11}C]MRB (Gallezot et al., 2011) and (S,S)-[^{18}F] FMeNER-D$_2$ (Seneca et al., 2006). This was also demonstrated for clomipramine, a TCA, using (S,S)-[^{18}F] FMeNER-D$_2$ in a monkey study (Takano et al., 2011). We previously reported NET occupancies by nortriptyline in healthy human volunteers (Sekine et al., 2010), and in patients with major depressive disorder (MDD) by milnacipran (Nogami et al., 2013), a serotonin norepinephrine reuptake inhibitor (SNRI), using (S,S)-[^{18}F] FMeNER-D$_2$.

The current study aimed to measure NET occupancies in the brain of patients with MDD taking various clinical doses of nortriptyline by using PET with (S,S)-[^{18}F] FMeNER-D$_2$. This is because our previous nortriptyline study only included normal volunteers with single oral administration, and we were unable to investigate the effects of high doses for ethical reasons. Moreover, there has been no report of NET occupancy in patients treated with relatively NET-selective antidepressants. Therefore, in this study, we explored the relationship between clinical daily doses of nortriptyline and its plasma concentrations, and central NET occupancies in MDD patients. We further estimated the NET occupancy corresponding to the reported minimum therapeutic level of plasma nortriptyline (Baumann et al., 2004, 2005; Hiemke et al., 2011).

Method

Subjects

Ten patients (8 men and 2 women; mean age, 40.1 yr; standard deviation [s.d.], 8.4 yr; range, 28–55 yr) fulfilling the Diagnostic and Statistical Manual of Mental Disorders IV (DSM-IV) criteria for MDD were recruited from facilitated psychiatric hospitals and clinics. They had no other history of major medical illnesses. All patients were taking a variety of clinical doses of nortriptyline (mean, 122.5 mg/d; s.d., 39.9 mg/d; range, 75–200 mg/d) as an antidepressant. No other antidepressants were used, but some of them were taking benzodiazepines for anxiety or insomnia. Experienced psychiatrists evaluated the patients' symptoms using the 21-item Hamilton Rating Scale for Depression (HAM-D) on the same day as the PET examinations. All of the patients were considered as responders to nortriptyline treatment with a mean HAM-D score of 7.3 (s.d., 4.7), and they had taken the drug for at least 1 month.

Age-matched healthy subjects (8 men and 3 women; mean, 39.6 yr; s.d., 9.1 yr; range, 23–55 yr) participated in the study as a control group. All healthy subjects were free of any somatic, neurological, or psychiatric disorders, and they had no history of current or previous drug abuse.

Studies were performed and analyzed at the National Institute of Radiological Sciences (NIRS, Japan). All participants provided written informed consent before participating in the study, which was approved by the Ethics and Radiation Safety Review board at NIRS.

PET procedures

(S,S)-[^{18}F]FMeNER-D$_2$ was synthesized by fluoromethylation of nor-ethyl-reboxetine with ^{18}F-bromofluoromethane-d$_2$ as previously described (Schou et al., 2004), yielding a radiochemical purity of higher than 95%.

An ECAT EXACT HR+ (CTI-Siemens, USA) PET scanner system was used with a head fixation device (Fixter, Sweden) to minimize head movement. A transmission scan for attenuation correction was performed using a ^{68}Ge-^{68}Ga source.

After an intravenous bolus injection of (S,S)-[^{18}F] FMeNER-D$_2$, regional brain radioactivity was measured from 120 to 180 min (10 min×6 frames). Injected radioactivity averaged 188.3 (s.d., 4.4) MBq for the patient group and 190.5 (s.d., 5.9) MBq for the reference group, and specific radioactivity averaged 255.2 (s.d., 155.3) GBq/μmol for the patient group and 295.8 (s.d., 180.2) GBq/μmol for the reference group at the time of injection.

Magnetic resonance (MR) images of the brain were acquired with a 1.5 Tesla MR scanner, Gyroscan NT (Philips Medical Systems, The Netherlands). Three-dimensional volumetric acquisition of a T1-weighted gradient echo sequence produced a gapless series of thin transverse sections (TE: 9.2 ms; TR: 21 ms; flip angle: 30 degrees; field of view: 256 mm; acquisition matrix: 256 × 256; slice thickness: 1 mm). The MRI results revealed no apparent structural abnormalities.

Plasma concentration of nortriptyline

Venous blood samples were taken to measure the plasma concentrations of nortriptyline just before and after the PET scan. The average values of these two samples were used in this study. The plasma concentrations
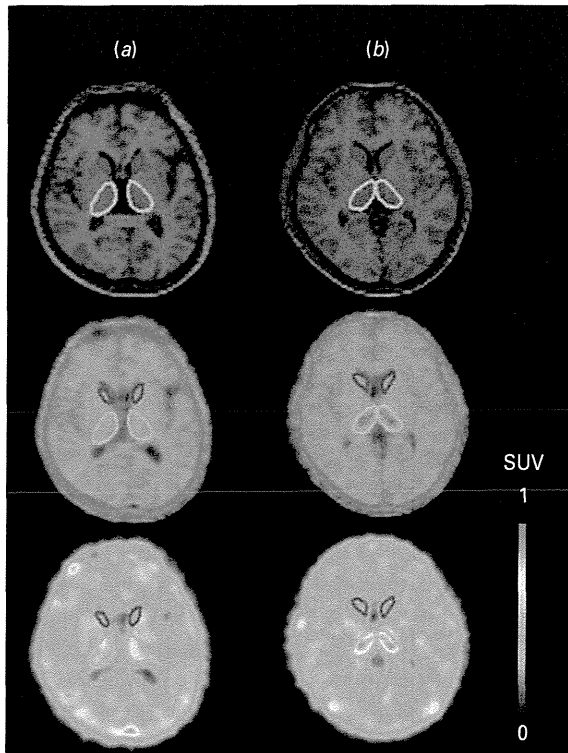
Fig. 1. Magnetic resonance imaging (MRI) and positron emission tomography (PET) images of a patient taking 150 mg/d of nortriptyline (*a*), and a normal subject not taking any drugs (*b*). The upper row shows MRI images, the middle row shows fused images of both the MRI and PET summated image, and the lower row shows PET summated images of the subjects. Examples of volumes of interest for the caudate nucleus and thalamus are also displayed. The color bar indicates standard uptake value (SUV).

of nortriptyline were determined by gas chromatography-mass spectrometry with a lower limit of quantification of 20.0 ng/ml (Mitsubishi Chemical Medience Corporation, Japan).

Data analyses

All emission scans were reconstructed with a Hanning filter (cutoff frequency: 0.4 cycle/pixel). All MR images were coregistered to the PET images using the software package PMOD (PMOD Technologies, Switzerland). Volumes of interest were drawn manually on summed PET images with reference to coregistered MR images, and were defined for the thalamus and caudate on three consecutive slices in the transverse plane (Fig. 1). Regional radioactivity was calculated for each frame, corrected for decay, and plotted *vs.* time.

(S,S)-[^{18}F]FMeNER-D$_2$ bindings were expressed as binding potentials relative to non-displaceable binding (BP$_{ND}$) (Innis et al., 2007). BP$_{ND}$ of (S,S)-[^{18}F] FMeNER-D$_2$ in the thalamus was calculated using the area under the curve (AUC) ratio method (Arakawa et al., 2008). We used the caudate as a reference brain

region because of its negligible NET density (Donnan et al., 1991; Schou et al., 2005; Logan et al., 2007). In the AUC ratio method, BP$_{ND}$ can be expressed as:

$$BP_{ND} = AUC_{thalamus}/AUC_{caudate} - 1,$$

where AUC$_{thalamus}$ is the area under the time–activity curve of the thalamus and AUC$_{caudate}$ is the area under the time–activity curve of the caudate. An integration interval of 120–180 min was used in this method.

The occupancies of NET were calculated by the following equation:

$$Occupancy(\%) = 100 \times (BP_{reference} - BP_{nortriptyline})/BP_{reference},$$

where BP$_{reference}$ is BP$_{ND}$ of the mean of age-matched healthy control subjects and BP$_{nortriptyline}$ is BP$_{ND}$ of the patients with nortriptyline treatment.

The relationships between dose or plasma concentration and occupancies of NET were modeled by the following equation:

$$Occupancy(\%) = 100 \times C/(E_{50} + C),$$

where C is the dose or plasma concentration of nortriptyline, and E$_{50}$ is the dose or plasma concentration required to induce 50% occupancy (Suhara et al., 2003; Takano et al., 2006).

Finally, we further explored the relationships between residual symptoms represented by HAM-D scores and the NET occupancies using Spearman's signed rank correlation. Total scores of 21-item HAM-D (HAM-D-21) and 6-item HAM-D (HAM-D-6: depressed mood, feelings of guilt, work and interests, general somatic symptoms, psychic , and psychomotor retardation) (Bech, 2006) extracted from HAM-D-21 were used for the correlation analysis. This is because HAM-D-6 has been reported to be more valid as an outcome measure to see the dose–response relationship than the full HAM-D in clinical trials of antidepressants (Bech et al., 2004, 2006). $P < 0.05$ was considered significant.

Results

Data of the healthy subjects and patients are listed in Tables 1 and 2, respectively. MRI and summated PET images of a patient taking 150 mg/d of nortriptyline and a normal subject are displayed in Fig. 1. The mean BP$_{ND}$ value of healthy subjects was 0.61. The relationships between the administered daily dose, or plasma concentration of nortriptyline, and NET occupancy in the thalamus are shown in Figs. 2 and 3. The estimated effective dose (ED$_{50}$) and concentration (EC$_{50}$) required to induce 50% NET occupancy were 65.9 mg/d and 79.8 ng/ml, respectively.

In respect of the relationships between residual symptoms and NET occupancies, we found no significant correlations between the total scores on the HAM-D-21 or HAM-D-6 and the NET occupancies in the thalamus

Table 1. Data of healthy control subjects

Healthy subjects	Gender	Age	BP_{ND}
1	F	23	0.69
2	M	32	0.54
3	M	33	0.68
4	M	34	0.58
5	M	39	0.62
6	F	39	0.63
7	M	40	0.56
8	M	43	0.54
9	M	49	0.71
10	F	49	0.68
11	M	55	0.49

BP_{ND}: BP_{ND} in the thalamus.

($\rho = -0.241$, $p=0.503$ for HAM-D-21 and $\rho = -0.338$, $p=0.340$ for HAM-D-6). Furthermore, no significant correlations were observed between the NET occupancies in the thalamus and the duration of illness or that of nortriptyline medication (duration of illness: $\rho = -0.248$, $p=0.489$ for HAM-D-21 and $\rho = -0.167$, $p=0.645$ for HAM-D-6; duration of nortriptyline medication: $\rho = 0.139$, $p=0.701$ for HAM-D-21 and $\rho = 0.025$, $p=0.946$ for HAM-D-6).

Discussion

In the present study, we investigated the occupancies of NET with various doses of nortriptyline, a drug that is chronically administered to patients with MDD. All of them were considered to be responders according to the in-charge physicians, and six of them were in remission (HAM-D $\leqslant$ 8). The results showed approximately 50–70% NET occupancies in the brain after the administration of 75–200 mg/d of nortriptyline.

Nortriptyline is a secondary amine TCA, and a NET-selective antidepressant that has more than 10-fold higher affinity to NET than 5-HTT (Owens et al., 1997; Frazer, 2000; Vaishnavi et al., 2004; Gillman, 2007). Although in recent years selective serotonin reuptake inhibitors (SSRIs) and SNRIs have been the first-line medications for MDD, TCAs have equivalent, or in some reports higher responder rates than SSRIs (Anderson, 1998, 2000; Nierenberg et al., 2003). Furthermore, along with desipramine, nortriptyline has the most pharmacologically desirable characteristics as a NET inhibitor, and it is also safe when co-administered with either monoamine oxidase inhibitors or SSRIs (Gillman, 2007). Thus, nortriptyline still commands an important role in the treatment of depression.

Previous PET studies have reported 5-HTT occupancy to be over 80% in patients with depression who have responded clinically to SSRIs (Meyer et al., 2001, 2004; Suhara et al., 2003). The same level of 5-HTT occupancy

was also reported with clomipramine (Suhara et al., 2003) and duloxetine (Takano et al., 2006) in terms of their clinical use for depression. Recently, Lundberg et al. (2012) demonstrated that patients in remission from depression showed lower than the proposed 80% 5-HTT occupancy associated with various antidepressants including TCAs (amitriptyline and clomipramine) and SSRIs (citalopram, fluoxetine, sertraline, and venlafaxine).

In contrast, there have been only a few studies to examine central NET occupancy by antidepressants. In our preliminary study of NET occupancy with nortriptyline for normal subjects (Sekine et al., 2010), we measured the NET occupancies resulting from single doses of nortriptyline (up to 75 mg) in 6 healthy young men, and found that ED_{50} was 76.8 mg and concentration (EC_{50}) was 59.8 ng/ml 5 h after a single oral administration. In our recent work, Nogami et al. (2013) examined both 5-HTT and NET occupancy in MDD patients treated with an SNRI, milnacipran. Estimated ED_{50} for 5-HTT was 122.5 and 149.9 mg for NET, and with milnacipran at 100 mg, the dose most commonly administered to MDD patients induces about 40% of occupancy in both 5-HTT and NET. However, it has been reported that higher doses of milnacipran such as 150 mg/d can lead to better improvement (Kanemoto et al., 2004; Hayashi et al., 2007).

With regard to nortriptyline, many previous investigations have suggested curvilinear relationships between plasma concentrations of nortriptyline and clinical response in patients with depression (Asberg et al., 1971; Sjoqvist et al., 1971; Sorensen et al., 1978; Perry et al., 1985, 1994; DeVane et al., 1991; Jerling et al., 1994), although some reported no correlation between the plasma nortriptyline levels and therapeutic effect (Burrows et al., 1972). As a result of this previous research, guidelines for therapeutic drug monitoring of psychotropic drugs (Baumann et al., 2004, 2005; Hiemke et al., 2011) claimed that the minimum therapeutic level of plasma nortriptyline was 70 ng/ml. Applying the data to the present study, our results indicate that this plasma nortriptyline concentration corresponds to 47% NET occupancy, suggesting that approximately 50% of central NET occupancy by nortriptyline would be necessary for the treatment of depression.

The ED_{50} and EC_{50} values in this study, i.e. 65.9 mg/d and 79.8 ng/ml, respectively, were different from those of our previous study (76.8 mg and 59.8 ng/ml, respectively) on healthy subjects (Sekine et al., 2010). The differences in ED_{50} and EC_{50} values between these two studies might be partly attributable to the different study protocols and different subjects: our current study involved chronic administration and depressed patients, whereas our previous study involved acute administration and healthy subjects. In addition, dose ranges were different between these two studies: our patients with depression were taking moderate-to-high doses of nortriptyline, whereas our previous study (Sekine et al., 2010) included

Table 2. Characteristics and results in patients with major depressive disorder (MDD)

Patients	Gender	Age	NTP dose (mg/d)	NTP plasma conc. (ng/ml)	BP_{ND}	HAM-D-21	HAM-D-6	DOI (M)	D-NTP (D)	Previous AD
1	F	38	75	117	0.24	8	3	32	75	None
2	M	28	75	53.8	0.29	11	5	55	412	PAX, MIL
3	M	55	100	93.7	0.24	4	3	10	38	MAP, PAX
4	M	43	100	111.8	0.19	1	1	19	101	PAX
5	M	34	100	175.4	0.25	14	6	28	386	SER, PAX
6	M	30	125	126.1	0.18	13	6	9	87	SER, MIL
7	M	50	150	165.5	0.26	6	4	32	51	PAX, FLV, SER
8	F	40	150	320.6	0.20	7	4	62	312	AMO
9	M	44	150	270.6	0.18	9	3	21	160	PAX, MIL, CLM, MIA
10	M	39	200	279.4	0.21	0	0	100	450	MIL

F: female; M: male; NTP: nortriptyline; Conc.: concentration; BP_{ND}: BP_{ND} in the thalamus; HAM-D-21: total score of 21-item Hamilton Depression Scale; HAM-D-6: total score of 6-item Hamilton Depression Scale; DOI: duration of illness (months); D-NTP: duration of nortriptyline medication (days); AD: antidepressants; PAX: paroxetine; MIL: milnacipran; MAP: maprotiline; SER: sertraline; FLV: fluvoxamine; AMO: amoxapine; CLM: clomipramine; MIA: mianserin.
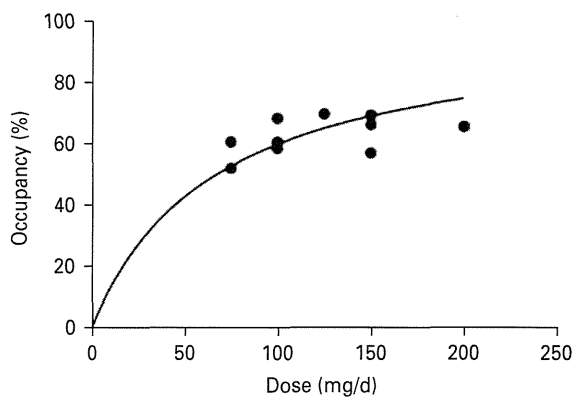

Fig. 2. The relationship between daily administered dose and norepinephrine transporter occupancy in the thalamus.
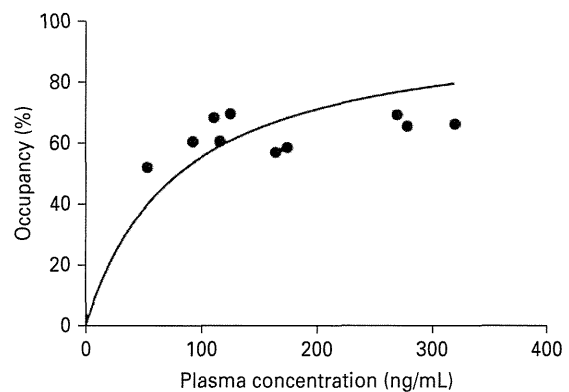

Fig. 3. The relationship between plasma concentration of nortriptyline and norepinephrine transporter occupancy.

healthy volunteers taking only low doses of nortriptyline for ethical reasons, which might cause different curve fitting.

We found no correlation between HAM-D-21 and HAM-D-6 total scores and NET occupancies, which may imply that depressive symptoms associated with norepinephrine, have been resolved in our responders to nortriptyline treatment, and the residual symptoms might be related to other factors, including different molecular systems. However, our current study evaluated patients only at one point in the responding phase of nortriptyline treatment, and further studies are needed on the change of symptoms in relation with NET occupancy.

There are several limitations in this study. First, we recruited patients with MDD chronically treated with nortriptyline, and we used the data from healthy subjects as reference BP_{ND}. An autoradiography study reported a reduction in NET in the locus coeruleus (LC) in patients with depression (Klimek et al., 1997); however, no PET

study has reported a comparison of NET BP_{ND} between patients with MDD before treatment and normal controls. This could cause over- and under-estimation of occupancies. Second, we included patients with different durations of nortriptyline medication, ranging from 38 to 450 d. We cannot exclude the possibility that different periods of medication can cause different functional changes in NET, since down-regulation (Bauer and Tejani-Butt, 1992; Zhu and Ordway, 1997; Zhu et al., 1998; Zavosh et al., 1999; Benmansour et al., 2004) as well as up-regulation (Biegon, 1986; Shores et al., 1994) and no change (Cheetham et al., 1996) of the transporter have all been reported in animal studies with chronic administration of NET inhibitors such as desipramine. However, for example, it was reported that such a down-regulation occurs at earlier stages of treatment and the change reached a maximal change after 3 wk, with no further down-regulation (Benmansour et al., 2004). Thus, the range of duration of medication with

nortriptyline in our study (38–450 d) may not have had a large effect on NET function, if it is present at all. Nevertheless, there has been no *in vivo* human study on the change in NET function after chronic administration of a NET inhibitor. In addition, the involvement of NET in the symptomatology, as well as the pathophysiology of MDD, should be explored in detail by a prospective study examining unmedicated patients with MDD and the time-course of treatment.

Finally, because an age-related decline of NET BP_{ND} (Ding et al., 2010) has been reported, we took it into consideration in the current study. However, the gender effect on NET BP_{ND} is not clear and has to be clarified in future.

In conclusion, we measured NET occupancies in MDD patients treated with nortriptyline, a relatively NET-selective TCA, using PET with (S,S)-[^{18}F]FMeNER-D$_2$. NET occupancy was approximately 50–70% at daily doses of 75–200 mg. Considering the reported minimum therapeutic level of plasma nortriptyline, more than 50% of central NET occupancy would be appropriate for the nortriptyline maintenance treatment of patients with MDD.

Statement of Interest

The authors declare that no financial support or compensation has been received from any individual or corporate entity for research or professional service, and there is no personal financial holding that could be perceived as constituting a potential conflict of interest.

References

Anderson IM (1998) SSRIS *vs.* tricyclic antidepressants in depressed inpatients: a meta-analysis of efficacy and tolerability. Depress Anxiety 7(Suppl. 1):11–17.

Anderson IM (2000) Selective serotonin reuptake inhibitors *vs.* tricyclic antidepressants: a meta-analysis of efficacy and tolerability. J Affect Disord 58:19–36.

Arakawa R, Okumura M, Ito H, Seki C, Takahashi H, Takano H, Nakao R, Suzuki K, Okubo Y, Halldin C, Suhara T (2008) Quantitative analysis of norepinephrine transporter in the human brain using PET with (S,S)-^{18}F-FMeNER-D$_2$. J Nucl Med 49:1270–1276.

Asberg M, Cronholm B, Sjoqvist F, Tuck D (1971) Relationship between plasma level and therapeutic effect of nortriptyline. Br Med J 3:331–334.

Bauer ME, Tejani-Butt SM (1992) Effects of repeated administration of desipramine or electroconvulsive shock on norepinephrine uptake sites measured by [^{3}H]nisoxetine autoradiography. Brain Res 582:208–214.

Baumann P, Hiemke C, Ulrich S, Eckermann G, Gaertner I, Gerlach M, Kuss HJ, Laux G, Muller-Oerlinghausen B, Rao ML, Riederer P, Zernig G, Arbeitsgemeinschaft fur Neuropsychopharmakologie und Pharmakopsychiatrie – Therapeutic Drug Monitoring group (2004) The AGNP-TDM expert group consensus guidelines: therapeutic drug monitoring in psychiatry. Pharmacopsychiatry 37:243–265.

Baumann P, Ulrich S, Eckermann G, Gerlach M, Kuss HJ, Laux G, Muller-Oerlinghausen B, Rao ML, Riederer P, Zernig G, Hiemke C, Arbeitsgemeinschaft fur Neuropsychopharmakologie und Pharmakopsyhiatrie – Therapeutic Drug Monitoring group (2005) The AGNP-TDM Expert Group Consensus Guidelines: focus on therapeutic monitoring of antidepressants. Dialogues Clin Neurosci 7:231–247.

Bech P (2006) Rating scales in depression: limitations and pitfalls. Dialogues Clin Neurosci 8:207–215.

Bech P, Tanghoj P, Cialdella P, Andersen HF, Pedersen AG (2004) Escitalopram dose–response revisited: an alternative psychometric approach to evaluate clinical effects of escitalopram compared to citalopram and placebo in patients with major depression. Int J Neuropsychopharmacol 7:283–290.

Bech P, Kajdasz DK, Porsdal V (2006) Dose–response relationship of duloxetine in placebo-controlled clinical trials in patients with major depressive disorder. Psychopharmacology (Berl) 188:273–280.

Benmansour S, Altamirano AV, Jones DJ, Sanchez TA, Gould GG, Pardon MC, Morilak DA, Frazer A (2004) Regulation of the norepinephrine transporter by chronic administration of antidepressants. Biol Psychiatry 55:313–316.

Biegon A (1986) Effect of chronic desipramine treatment on dihydroalprenolol, imipramine, and desipramine binding sites: a quantitative autoradiographic study in the rat brain. J Neurochem 47:77–80.

Brunello N, Mendlewicz J, Kasper S, Leonard B, Montgomery S, Nelson J, Paykel E, Versiani M, Racagni G (2002) The role of noradrenaline and selective noradrenaline reuptake inhibition in depression. Eur Neuropsychopharmacol 12:461–475.

Burrows GD, Davies B, Scoggins BA (1972) Plasma concentration of nortriptyline and clinical response in depressive illness. Lancet 2:619–623.

Cheetham SC, Viggers JA, Butler SA, Prow MR, Heal DJ (1996) [^{3}H]nisoxetine – a radioligand for noradrenaline reuptake sites: correlation with inhibition of [^{3}H]noradrenaline uptake and effect of DSP-4 lesioning and antidepressant treatments. Neuropharmacology 35:63–70.

Dell'Osso B, Palazzo MC, Oldani L, Altamura AC (2011) The noradrenergic action in antidepressant treatments: pharmacological and clinical aspects. CNS Neurosci Ther 17:723–732.

DeVane CL, Rudorfer MV, Potter WZ (1991) Dosage regimen design for cyclic antidepressants: a review of pharmacokinetic methods. Psychopharmacol Bull 27:619–631.

Ding YS, Singhal T, Planeta-Wilson B, Gallezot JD, Nabulsi N, Labaree D, Ropchan J, Henry S, Williams W, Carson RE, Neumeister A, Malison RT (2010) PET imaging of the effects of age and cocaine on the norepinephrine transporter in the human brain using (S,S)-[^{11}C]O-methylreboxetine and HRRT. Synapse 64:30–38.

Donnan GA, Kaczmarczyk SJ, Paxinos G, Chilco PJ, Kalnins RM, Woodhouse DG, Mendelsohn FA (1991) Distribution of catecholamine uptake sites in human brain as determined by quantitative [^{3}H] mazindol autoradiography. J Comp Neurol 304:419–434.

Frazer A (2000) Norepinephrine involvement in antidepressant action. J Clin Psychiatry 61(Suppl. 10):25–30.

Frazer A (2001) Serotonergic and noradrenergic reuptake inhibitors: prediction of clinical effects from in vitro potencies. J Clin Psychiatry 62(Suppl. 12):16–23.

Gallezot JD, Weinzimmer D, Nabulsi N, Lin SF, Fowles K, Sandiego C, McCarthy TJ, Maguire RP, Carson RE, Ding YS (2011) Evaluation of [^{11}C]MRB for assessment of occupancy of norepinephrine transporters: studies with atomoxetine in non-human primates. NeuroImage 56:268–279.

Gillman PK (2007) Tricyclic antidepressant pharmacology and therapeutic drug interactions updated. Br J Pharmacol 151:737–748.

Harald B, Gordon P (2012) Meta-review of depressive subtyping models. J Affect Disord 139:126–140.

Hayashi M, Mimura M, Otsubo T, Kamijima K (2007) Effect of high-dose milnacipran in patients with depression. Neuropsychiatr Dis Treat 3:699–702.

Hiemke C et al. (2011) AGNP consensus guidelines for therapeutic drug monitoring in psychiatry: update 2011. Pharmacopsychiatry 44:195–235.

Innis RB et al. (2007) Consensus nomenclature for in vivo imaging of reversibly binding radioligands. J Cereb Blood Flow Metab 27:1533–1539.

Jerling M, Merle Y, Mentre F, Mallet A (1994) Population pharmacokinetics of nortriptyline during monotherapy and during concomitant treatment with drugs that inhibit CYP2D6 – an evaluation with the nonparametric maximum likelihood method. Br J Clin Pharmacol 38:453–462.

Kanemoto K, Matsubara M, Yamashita K, Tarao Y, Inada E, Sekine T (2004) Controlled comparison of two different doses of milnacipran in major depressive outpatients. Int Clin Psychopharmacol 19:343–346.

Kasper S, Meshkat D, Kutzelnigg A (2011) Improvement of the noradrenergic symptom cluster following treatment with milnacipran. Neuropsychiatr Dis Treat 7:21–27.

Klimek V, Stockmeier C, Overholser J, Meltzer HY, Kalka S, Dilley G, Ordway GA (1997) Reduced levels of norepinephrine transporters in the locus coeruleus in major depression. J Neurosci 17:8451–8458.

Logan J, Wang GJ, Telang F, Fowler JS, Alexoff D, Zabroski J, Jayne M, Hubbard B, King P, Carter P, Shea C, Xu Y, Muench L, Schlyer D, Learned-Coughlin S, Cosson V, Volkow ND, Ding YS (2007) Imaging the norepinephrine transporter in humans with (S,S)-[^{11}C]O-methyl reboxetine and PET: problems and progress. Nucl Med Biol 34:667–679.

Lundberg J, Tiger M, Landen M, Halldin C, Farde L (2012) Serotonin transporter occupancy with TCAs and SSRIs: a PET study in patients with major depressive disorder. Int J Neuropsychopharmacol 15:1167–1172.

Meyer JH, Wilson AA, Ginovart N, Goulding V, Hussey D, Hood K, Houle S (2001) Occupancy of serotonin transporters by paroxetine and citalopram during treatment of depression: a [^{11}C]DASB PET imaging study. Am J Psychiatry 158:1843–1849.

Meyer JH, Wilson AA, Sagrati S, Hussey D, Carella A, Potter WZ, Ginovart N, Spencer EP, Cheok A, Houle S (2004) Serotonin transporter occupancy of five selective serotonin reuptake inhibitors at different doses: an [^{11}C]DASB positron emission tomography study. Am J Psychiatry 161:826–835.

Nestler E, Hyman S, Malenka R (2008) Molecular neuro-pharmacology: a foundation for clinical neuroscience, Second Edition. McGraw-Hill Professional, New York.

Nierenberg AA, Papakostas GI, Petersen T, Kelly KE, Iacoviello BM, Worthington JJ, Tedlow J, Alpert JE, Fava M (2003) Nortriptyline for treatment-resistant depression. J Clin Psychiatry 64:35–39.

Nogami T, Takano H, Arakawa R, Ichimiya T, Fujiwara H, Kimura Y, Kodaka F, Sasaki T, Takahata K, Suzuki M, Nagashima T, Mori T, Shimada H, Fukuda H, Sekine M, Tateno A, Takahashi H, Ito H, Okubo Y, Suhara T (2013) Occupancy of serotonin and norepinephrine transporter by milnacipran in patients with major depressive disorder: a positron emission tomography study with [^{11}C]DASB and (S,S)-[^{18}F]FMeNER-D$_2$. Int J Neuropsychopharmacol 16:937–943.

Owens MJ, Morgan WN, Plott SJ, Nemeroff CB (1997) Neurotransmitter receptor and transporter binding profile of antidepressants and their metabolites. J Pharmacol Exp Ther 283:1305–1322.

Perry PJ, Browne JL, Alexander B, Pfohl BM, Dunner FJ, Sherman AD, Tsuang MT (1985) Relationship of free nortriptyline levels to therapeutic response. Acta Psychiatr Scand 72:120–125.

Perry PJ, Zeilmann C, Arndt S (1994) Tricyclic antidepressant concentrations in plasma: an estimate of their sensitivity and specificity as a predictor of response. J Clin Psychopharmacol 14:230–240.

Schou M, Halldin C, Sovago J, Pike VW, Hall H, Gulyas B, Mozley PD, Dobson D, Shchukin E, Innis RB, Farde L (2004) PET evaluation of novel radiofluorinated reboxetine analogs as norepinephrine transporter probes in the monkey brain. Synapse 53:57–67.

Schou M, Halldin C, Pike VW, Mozley PD, Dobson D, Innis RB, Farde L, Hall H (2005) Post-mortem human brain autoradio-graphy of the norepinephrine transporter using (S,S)-[^{18}F] FMeNER-D$_2$. Eur Neuropsychopharmacol 15:517–520.

Sekine M, Arakawa R, Ito H, Okumura M, Sasaki T, Takahashi H, Takano H, Okubo Y, Halldin C, Suhara T (2010) Norepinephrine transporter occupancy by antidepressant in human brain using positron emission tomography with (S,S)-[^{18}F]FMeNER-D$_2$. Psychopharmacology 210:331–336.

Seneca N, Gulyas B, Varrone A, Schou M, Airaksinen A, Tauscher J, Vandenhende F, Kielbasa W, Farde L, Innis RB,

Halldin C (2006) Atomoxetine occupies the norepinephrine transporter in a dose-dependent fashion: a PET study in nonhuman primate brain using (S,S)-[^{18}F]FMeNER-D$_2$. Psychopharmacology (Berl) 188:119–127.

Shores MM, Szot P, Veith RC (1994) Desipramine-induced increase in norepinephrine transporter mRNA is not mediated via alpha 2 receptors. Brain Res Mol Brain Res 27:337–341.

Sjoqvist F, Alexanderson B, Asberg M, Bertilsson L, Borga O, Hamberger B, Tuck D (1971) Pharmacokinetics and biological effects of nortriptyline in man. Acta Pharmacol Toxicol (Copenh) 29(Suppl. 3):255–280.

Sorensen B, Kragh-Sorensen P, Larsen NE, Hvidberg EF (1978) The practical significance of nortriptyline plasma control: a prospective evaluation under routine conditions in endogenous depression. Psychopharmacology (Berl) 59:35–39.

Suhara T, Takano A, Sudo Y, Ichimiya T, Inoue M, Yasuno F, Ikoma Y, Okubo Y (2003) High levels of serotonin transporter occupancy with low-dose clomipramine in comparative occupancy study with fluvoxamine using positron emission tomography. Arch Gen Psychiatry 60:386–391.

Takano A, Suzuki K, Kosaka J, Ota M, Nozaki S, Ikoma Y, Tanada S, Suhara T (2006) A dose-finding study

of duloxetine based on serotonin transporter occupancy. Psychopharmacology (Berl) 185:395–399.

Takano A, Nag S, Gulyas B, Halldin C, Farde L (2011) NET occupancy by clomipramine and its active metabolite, desmethylclomipramine, in non-human primates in vivo. Psychopharmacology (Berl) 216:279–286.

Uher R et al. (2009) Differential efficacy of escitalopram and nortriptyline on dimensional measures of depression. Br J Psychiatry 194:252–259.

Vaishnavi SN, Nemeroff CB, Plott SJ, Rao SG, Kranzler J, Owens MJ (2004) Milnacipran: a comparative analysis of human monoamine uptake and transporter binding affinity. Biol Psychiatry 55:320–322.

Zavosh A, Schaefer J, Ferrel A, Figlewicz DP (1999) Desipramine treatment decreases ^{3}H-nisoxetine binding and norepinephrine transporter mRNA in SK-N-SHSY5Y cells. Brain Res Bull 49:291–295.

Zhu MY, Ordway GA (1997) Down-regulation of norepinephrine transporters on PC12 cells by transporter inhibitors. J Neurochem 68:134–141.

Zhu MY, Blakely RD, Apparsundaram S, Ordway GA (1998) Down-regulation of the human norepinephrine transporter in intact 293-hNET cells exposed to desipramine. J Neurochem 70:1547–1555.

OXFORD
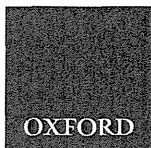
RESEARCH ARTICLE

Quantification of Central Substance P Receptor Occupancy by Aprepitant Using Small Animal Positron Emission Tomography

Tadashi Endo, MSc; Takeaki Saijo, PhD; Eisuke Haneda, PhD; Jun Maeda, PhD; Masaki Tokunaga, PhD; Ming-Rong Zhang, PhD; Ayako Kannami, BSc; Hidetoshi Asai, PhD; Masayuki Suzuki, MSc; Tetsuya Suhara, MD, PhD; Makoto Higuchi, MD, PhD

Molecular Imaging Center, National Institute of Radiological Sciences, Chiba, Japan (Drs Endo, Saijo, Haneda, Maeda, Tokunaga, Zhang, Suhara, Higuchi); Department of Molecular Neuroimaging, Tohoku University Graduate School of Medicine, Sendai, Japan (Drs Endo, Saijo, Suhara, and Higuchi); DMPK Research Laboratory, Mitsubishi Tanabe Pharma Corporation, Kisarazu, Japan (Drs Endo, Saijo, and Kannami); Clinical & Research Quality Assurance Department, Mitsubishi Tanabe Pharma Corporation, Tokyo, Japan (Dr Asai); Clinical Pharmacology Department, Mitsubishi Tanabe Pharma Corporation, Tokyo, Japan (Dr Suzuki).

Correspondence: Makoto Higuchi, MD, PhD, Molecular Imaging Center, National Institute of Radiological Sciences, 4-9-1 Anagawa, Inage-ku, Chiba, Chiba 263–8555, Japan (mhiguchi@nirs.go.jp).

Abstract

Background: Central substance P receptors, termed NK-1 receptors, have been considered as therapeutic targets in the development of drugs against diverse conditions, including emesis, overactive bladder, and depression.
Methods: Here, we applied small animal positron emission tomography (PET) and a radioligand for NK-1 receptors ([^{18}F]FE-SPA-RQ) for measuring occupancies of these receptors by a selective antagonist (aprepitant) in order to examine the validity of this in vivo imaging system for preclinical characterization of candidate agents acting on NK-1 receptors, and as a tool for predicting optimal doses in humans.
Results: PET in gerbils depicted high uptake in the striatum and dose-dependent displacement with increasing doses of aprepitant. Occupancies increased as a function of aprepitant plasma concentrations according to a one-site competition model, which agrees with reported occupancy-concentration relationships in clinical studies after correction for species differences in plasma protein-unbound aprepitant fractions. These occupancy data were further supported by ex vivo autoradiography of brain samples from aprepitant-treated gerbils. In a pilot study of a marmoset, we obtained more accurate determinations of NK-1 receptor occupancy, less affected by spillover of signals from extracranial tissues than in gerbil experiments.
Conclusions: These findings support the utility of small animals and quantitative PET in the development of drugs targeting NK-1 receptors.

Keywords: NK-1 receptor, receptor occupancy, small-animal PET, substance P

1

Introduction

Tachykinins are a family of neuropeptides carrying C-terminal Phe-X-Gly-Leu-Met-NH2. Substance P, neurokinin A, and neurokinin B are mammalian tachykinins that bind to NK-1, NK-2, and NK-3 receptors, respectively, with high affinity. The NK-1 receptor is a seven-transmembrane G protein-coupled receptor that is widely expressed in the central nervous system (Nakanishi, 1991; Otsuka and Yoshioka, 1993). A previous assay of human brain sections documented that high-level expression of NK-1 receptors is localized in brain areas involved in the regulation of affective behaviors, including the locus coeruleus, periaqueductal gray area, caudate, putamen, nucleus accumbens, nucleus of the diagonal band, and septum (Rigby et al., 2005). It was also reported that NK-1 receptors were expressed in the areas of the postrema and nucleus tractus solitaries, which are involved in emetic reflex (McRitchie et al., 1994; Rigby et al., 2005), and immunohistochemical analyses of the monkey brain demonstrated the presence of NK-1 receptors in the substantia nigra (Lévesque et al., 2007), which is known to be involved in Parkinson's disease. Substance P is distributed in the amygdala, hypothalamus, hippocampus, and striatum of rodent and primate brains (Hayashi, 1992; Jakab et al., 1996; Ribeiro & Hökfelt, 2000). In the striatum, substance P is primarily contained in a significant population of medium spiny neurons, which are major striatal projection neurons (Aosaki and Kawaguchi, 1996); substance P–containing medium spiny neurons are considered to receive corticostriatal inputs (Reiner et al., 2010) and to form synapses with other medium spiny neurons (Blomeley et al., 2009). This implies that substance P and NK-1 receptors modulate corticostriatal processing, which may be responsible for corticostriatal dysfunction in schizophrenia (Zandbelt et al., 2011).

The characteristic regional and cellular localizations of substance P and NK-1 receptors are indeed associated with reported pathophysiological roles of these neurotransmission components in pain (Snider and McMahon, 1998), vomiting (Sanger, 2004), inflammation (Kincy-Cain et al., 1996; Metwali et al., 2004), overactive bladder (Lecci and Maggi, 2001), depression (Kramer et al., 1998, 2004), schizophrenia (Tooney et al., 2001, 2006), Parkinson's disease (Rioux and Joyce, 1993), and alcoholism (George et al., 2008). Thus, NK-1 receptor antagonists are of potential importance for treating these conditions. Aprepitant (EMEND®), a selective and potent brain-permeable non-peptide NK-1 receptor antagonist with an IC_{50} of 100 pM (Tattersall et al., 2000; Bergström et al., 2004), is used to prevent vomiting and retching induced by anticancer agents. The therapeutic efficacy of aprepitant against overactive bladder has also been reported in a clinical trial for postmenopausal women (Green et al., 2006). Although exploratory clinical studies indicated antidepressant activity of aprepitant (Kramer et al., 1998, 2004), a Phase III clinical trial failed to prove its efficacy for major depression (Keller et al., 2006).

As a non-peptide positron emission tomography (PET) ligand with brain permeability, [18F]2-fluoromethoxy-5-(5-trifluoromethyl-tetrazol-1-yl)-benzyl([2S,3S]2-phenylpiperidin-3-yl)-amine ([18F]SPA-RQ) has been used in humans to evaluate the occupancy of the NK-1 receptor by a drug in clinical studies (Bergström et al., 2004; Hietala et al., 2005; Yasuno et al., 2007). Analyses of human studies with this tracer were compromised by high uptake of radioactivity in the skull, presumably due to metabolic liberation of 18F-fluoride, which is trapped in osseous tissue (Hietala et al., 2005).

In order to minimize the problems arising from de-fluorination in vivo, a new PET ligand, [18F]fluoroethoxy-SPA-RQ ([18F]-FE-SPA-RQ), was developed for visualization of central NK-1 receptors, and its use in both non-clinical and clinical studies (Haneda et al., 2007; Okumura et al., 2008) has been reported. [18F]-FE-SPA-RQ has a higher affinity for the human-type NK-1 receptor than [18F]SPA-RQ, and it yields only low-level accumulation of radioactivity in the skull (Haneda et al., 2007). Here, we measured central NK-1 receptor occupancy by aprepitant using small animal PET with [18F]FE-SPA-RQ, based on an analytical model assuming one-site competition between aprepitant and [18F]FE-SPA-RQ. The translatability of relationships between the plasma concentration of aprepitant and its NK-1 receptor occupancy from animals to humans was then assessed by comparing the present data to reported clinical values. We employed gerbils and a common marmoset for the current assays because these animals express NK-1 receptors that are pharmacologically similar to those in humans (Fong et al., 1992; Haneda et al., 2007).

Materials and Methods

Animals

The present research protocols were approved by the Animal Ethics Committees of the National Institute of Radiological Sciences and Mitsubishi Tanabe Pharma Corporation, and were performed in accordance with the Principles of Laboratory Animal Care (NIH publication no. 85-23, revised 1985).

Male Mongolian gerbils weighing 60–85 g were purchased from Japan SLC and kept in animal rooms maintained at 24°C, with a 12-h light/dark cycle and food and water ad libitum. A 6-year-old male marmoset weighing 430 g was obtained from CLEA Japan and used for in vivo PET experiments.

Generation of Template Anatomical Images

Prior to PET measurements, neuroanatomical template images of the gerbil brain were generated using a high-resolution magnetic resonance imaging (MRI) system, as previously described (Haneda et al., 2007). In brief, a gerbil was anesthetized with sodium pentobarbital and scanned with a 400 mm–bore, 7-Tesla horizontal magnet (NIRS/KOBELCO; Bruker BioSpin GmbH) equipped with 120-mm diameter gradients (Bruker BioSpin). Coronal T2-weighted MR images were obtained by fast spin-echo sequences with the following imaging parameters: repetition time = 4000 ms, effective echo time = 48 ms, field of view = 25 mm × 16 mm, nominal resolution = 117 μm × 117 μm, slice thickness = 600 μm, and number of averages = 32.

An anatomical template of the marmoset brain was also previously obtained from the embedded head using a 7-Tesla MRI system (National Institute of Radiological Sciences/KOBELCO/Bruker; Haneda et al., 2007). Coronal T2-weighted MR images were obtained by fast spin-echo sequences with the following imaging parameters: repetition time = 7000 ms, effective echo time = 45.8 ms, field of view = 40 mm × 40 mm, nominal resolution = 156 μm × 208 μm, slice thickness = 1000 μm, and number of averages = 24.

Radioligand Synthesis

The NK-1 receptor antagonist FE-SPA-RQ (molecular weight = 464) was labeled with positron emitter fluorine-18 (18F). Details of the precursor compound (Merck) and radiosynthesis

were described elsewhere (Hamill et al., 2003; Zhang et al., 2003). In brief, [^{18}F]FCH$_2$CH$_2$Br was prepared from [^{18}F]F$^-$ and 2-bromoethyl triflate, and was purified by distillation. Subsequently, ^{18}F-fluoroalkylation of the deprotonated phenolic hydroxyl group in the precursor with FCH$_2$CH$_2$Br in dimethyl formamide was performed at 120°C for 10 min. The resultant [^{18}F]FE-SPA-RQ was purified using preparative HPLC. The final product was formulated in saline solution (10 mL) containing Tween 80 (75 µL). The specific radioactivity of this radiotracer was 640±79 GBq/µmol (n = 18) at the end of synthesis.

PET Scans

A series of 6 dynamic PET scans was performed for each gerbil approximately 4 h after oral pretreatment with aprepitant (prepared by Mitsubishi Tanabe Pharma Corp.) at graded doses of 0.03, 0.1, 0.3, 3, and 30 mg/kg dissolved in 10% Gelucire. Individual PET scans for these gerbils (n = 6) were conducted at least 1 week apart. Complete recovery of [^{18}F]FE-SPA-RQ binding to a baseline level was confirmed after a 1-week washout of aprepitant in our initial pilot study. PET scans of the marmoset were carried out at baseline and 3 h after treatment with 20 mg/kg aprepitant delivered in dimethyl sulfoxide carrier by intravenous injection to the femoral vein.

PET for the marmoset and gerbils was performed using a small animal-dedicated microPET FOCUS220 system (Siemens Medical Solutions), which yields a 25.8 cm (transaxial) × 7.6 cm (axial) field of view and a spatial full-width resolution of 1.3 mm at half maximum in the center of the field of view (Tai et al., 2005). Anesthesia during the experiment was induced and maintained with 1.5–2% isoflurane in air (flow rate, 2 mL/min). Gerbils were kept warm using a small-animal warmer/thermometer system (BWT-100; Bio Research Center).

Prior to the PET scans of the gerbils, femoral veins were cannulated for injection of [^{18}F]FE-SPA-RQ and blood sampling. Dynamic scans were initiated at the time of a slow bolus [^{18}F]FE-SPA-RQ injection, and continued for 360 min. The injected dose of [^{18}F]FE-SPA-RQ was 35–55 MBq. All list-mode data were sorted into 3D sinograms, which were then Fourier-rebinned into 2D sinograms (frames: 4×1, 8×2, 14×5, and 27×10 min).

Prior to the PET scans of the marmoset, the cephalic vein was cannulated for radioligand injection. Dynamic scans were initiated at the time of a slow bolus [^{18}F]FE-SPA-RQ injection, and lasted for 180 min. The injected dose of [^{18}F]FE-SPA-RQ was 90–100 MBq. All list-mode data were sorted into 3D sinograms, which were then Fourier-rebinned into 2D sinograms (frames: 4×1, 8×2, 14×5, and 9×10 min).

Images were reconstructed from sonograms using 2D-filtered back projection with a 0.5-mm Hanning filter. Regions of interests (ROIs) were placed on the striatum and cerebellum on the anatomical MRI template. PET images of each animal were coregistered to the MRI template, and radioactivity in each ROI defined on the template was quantified using PMOD® software (PMOD Group).

In Vivo Quantification of [^{18}F]FE-SPA-RQ Binding and NK-1 Receptor Occupancy by Aprepitant

Specific binding of [^{18}F]FE-SPA-RQ was determined by estimating binding potential relative to nondisplaceable uptake (BP$_{ND}$) using a simplified reference tissue model (SRTM; Lammertsma et al., 1996) with PMOD® software (PMOD Group). We used the cerebellum as the reference brain region because of its negligible NK-1 receptor density. Assuming that target and reference

regions have the same levels of nondisplaceable binding, SRTM describes time–activity data in the target region as follows:

$$C_T(t) = R_1 C_R(t) + \left(K_2 - R_1 K_2 / [1 + BP_{ND}]\right) C_R(t)$$
$$\otimes \exp\left(--k_2 t / [1 + BP_{ND}]\right),$$

where R$_1$ is the ratio of K$_1$/K$_1'$ (K$_1$, influx rate constant for the target region; K$_1'$, influx rate constant for the reference region), C$_R$(t) is the radioactivity concentration in the reference region, and $\otimes$ denotes the convolution integral. Using this method, 3 parameters (R$_1$, k$_2$, and BP$_{ND}$) were estimated by the use of a nonlinear curve-fitting procedure. Scan data of 60, 120, 180, 240, 300, and 360 min were used.

NK-1 receptor occupancy (Occ) by aprepitant in each gerbil was determined according to the following equation:

$$Occ = \left(BP_{ND, untreated} - BP_{ND, drug}\right) / BP_{ND, untreated} \times 100,$$

where BP$_{ND, untreated}$ and BP$_{ND, drug}$ are BP$_{ND}$ values obtained by PET at baseline and after aprepitant administration, respectively.

In the marmoset, full occupancy of NK-1 receptors by 20 mg/kg of aprepitant was examined on the basis of radioligand retention at the end of PET as follows:

$$Occ = \left[\left(ID_{untreated} - ID_{drug}\right) / ID_{untreated}\right] \times 100,$$

where ID$_{untreated}$ and ID$_{drug}$ are specific radioligand bindings in the striatum 180 min after [^{18}F]FE-SPA-RQ administration at baseline and after aprepitant administration, respectively. Specific radioligand bindings were calculated by subtracting cerebellar radioactivity from striatal radioactivity and were expressed as a percentage of the injected radioligand dose per unit tissue volume (%dose/mL).

Ex Vivo Autoradiographic Measurement of NK-1 Receptor Occupancies

A group of gerbils distinct from those used for in vivo PET were prepared for ex vivo autoradiographic estimation of NK-1 receptor occupancies. After oral treatment with 3 different doses (0.3, 3, and 30 mg/kg) of aprepitant in 10% Gelucire solution, gerbils were sacrificed at various time points (0.5, 1, 2, 4, 8, and 24 h) by collecting whole blood from the postcaval vein under ether anesthesia. Each brain was rapidly removed, frozen with powdered dry ice, and sliced into 20-µm sections at –20°C using an HM560 cryostat microtome (Carl Zeiss). Sections were stored at –80°C until analysis. Autoradiography with [^{18}F]FE-SPA-RQ was conducted as described elsewhere (Haneda et al., 2007) except that we used 10 µM aprepitant instead of 1 µM SDZ NKT343 to abolish specific radioligand binding. Signal intensities in an ROI on the striatum were calculated using Multi Gauge software (Fuji Film), and specific radioligand binding was determined as the difference between signal intensities in the absence and presence of 10 µM aprepitant. NK-1 receptor occupancy by aprepitant was estimated according to the following equation:

$$Occ = \left(1 - RD_{drug} / RD_{untreated}\right) \times 100,$$

where RD$_{drug}$ and RD$_{untreated}$ are specific binding levels expressed as photo-stimulated luminescence per unit area (PSL/mm^2) in samples from gerbils treated with aprepitant and vehicle, respectively.

Analysis of Plasma Aprepitant Concentrations and their Correlation with NK-1 Receptor Occupancy

Acetonitrile was added to 50 µL of plasma samples from gerbils to remove proteins. In the *in vivo* PET study, plasma samples were collected just after the injection of [^{18}F]FE-SPA-RQ. In the *ex vivo* autoradiographic analyses, plasma aprepitant concentrations were determined using solid phase extraction by OASIS HLB (Waters) as an additional pretreatment analysis. The purified sample was then injected into a liquid chromatography–tandem mass spectrometry (LC/MS/MS) system. HPLC analysis was performed on an Xbridge C18 column (3.5 µm, 2.1×50 mm, Waters) at 40°C. The mobile phase comprised acetonitrile/water/formic acid (50/50/0.1, v/v/v), and was used at a flow rate of 0.5 mL/min. Eluted aprepitant was ionized using an electrospray interface and detected by multiple reaction monitoring of the transitions from 535 to 277. Samples from *ex vivo* autoradiographic studies were applied to an LC/MS/MS system comprising an LC-20AD pump (Shimadzu) controlled by an SCL-10Avp system controller (Shimadzu) and an API-4000 mass spectrometer (Applied Biosystems/MDS SCIEX). Plasma samples from the *in vivo* PET experiments were processed using Agilent 1100 (Agilent) and 4000QTRAP (Applied Biosystems/MDS SCIEX) systems.

The relationship between receptor occupancy and plasma drug concentrations at equilibrium between free drug compartments in the brain and plasma can be described using the following equation:

$$Occ = Occ_{max} \times C_p / (C_p + EC_{50}),$$

where Occ_{max} and C_p are the maximal receptor occupancy and plasma drug concentrations, respectively, and EC_{50} is the plasma drug concentration required for 50% Occ_{max}.

Plasma protein binding

Fractions of protein-bound aprepitant in human and gerbil plasma collected immediately after the injection of radioligand were measured by ultracentrifugation. Three hundred microliters of plasma samples were spiked into a standard solution containing 10 µg/mL aprepitant, with the final concentration then adjusted to 0.1 µg/mL at 4°C. Plasma samples were transferred in micro-tubes and centrifuged at 50 000 rpm at 4°C for 4 h. Plasma proteins were removed by adding 100 µL of acetonitrile to 10 and

20 µL of samples before ultracentrifugation to measure the total concentration of aprepitant. These samples were centrifuged at 13 000 rpm for 3 min at 4°C. To determine plasma aprepitant concentrations before and after ultracentrifugation, the supernatant was injected into the LC/MS/MS system and then assayed as described above. Plasma protein binding of aprepitant was calculated as follows:

$$\text{Protein binding } (\%) = (1 - C_u / C_p) \times 100,$$

where C_p and C_u were the plasma aprepitant concentration before and after ultracentrifugation, respectively.

Results

[^{18}F]FE-SPA-RQ-PET of Gerbil Striatal NK-1 Receptor Occupancy by Aprepitant

Dynamic PET experiments of gerbils were conducted for 6 h after intravenous injection of [^{18}F]FE-SPA-RQ to ensure achievement of a pseudo-equilibrium state of radioligand binding within this imaging time. In agreement with our previous study (Haneda et al., 2007), the highest and lowest radioligand retention was observed in the striatum and cerebellum, respectively, of gerbil brains, reflecting the distribution of central NK-1 receptors (Figure 1). Pretreatment of gerbils with aprepitant 4 h before initiation of PET attenuated striatal radioligand binding in a dose-dependent manner, whereas radioligand uptake and retention in the cerebellum remained unaltered (Figures 1 and 2). Marked nonspecific radioligand accumulation in Harderian glands (data not shown) resulted in the spillover of radioactivity into neighboring tissues, including the rostral striatum, irrespective of aprepitant pretreatment. Accordingly, striatal radioactivity even remained slightly higher than cerebellar radioactivity after treatment with excessive aprepitant (30 mg/kg; Figure 2F). Correspondingly, BP_{ND} of [^{18}F]FE-SPA-RQ in the striatum of gerbils treated with 30 mg/kg aprepitant was estimated as 0.27 using the cerebellum as reference (Table 1). Moreover, due to spillover of radioactivity from the Harderian glands, apparent maximal NK-1 receptor occupancy did not reach 100%. We then conducted a time-stability analysis of specific radioligand binding by assessing the effects of progressive truncation of PET data on the estimated BP_{ND} values (Figure 3A and B), and found that a 120 min scan could be sufficient for stable estimation of the
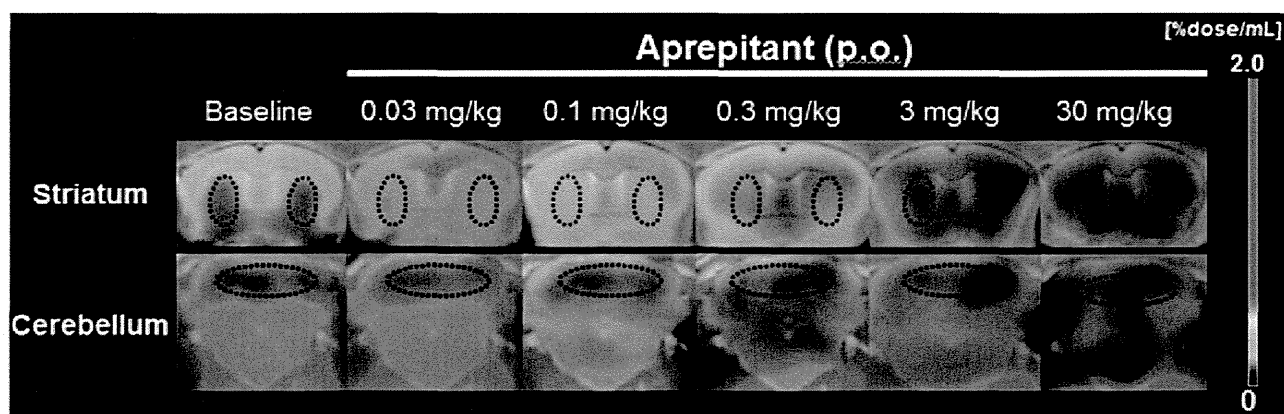

Figure 1. Representative coronal PET images showing [^{18}F]FE-SPA-RQ distribution in gerbil brains at baseline and after oral administration (per os; p. o.) of aprepitant. PET data were generated by summation of dynamic data at 0–6 h after intravenous radioligand injection, and were merged onto the MRI template. ROIs (outlined by dots) were placed on the striatum (upper row) and cerebellum (lower row).
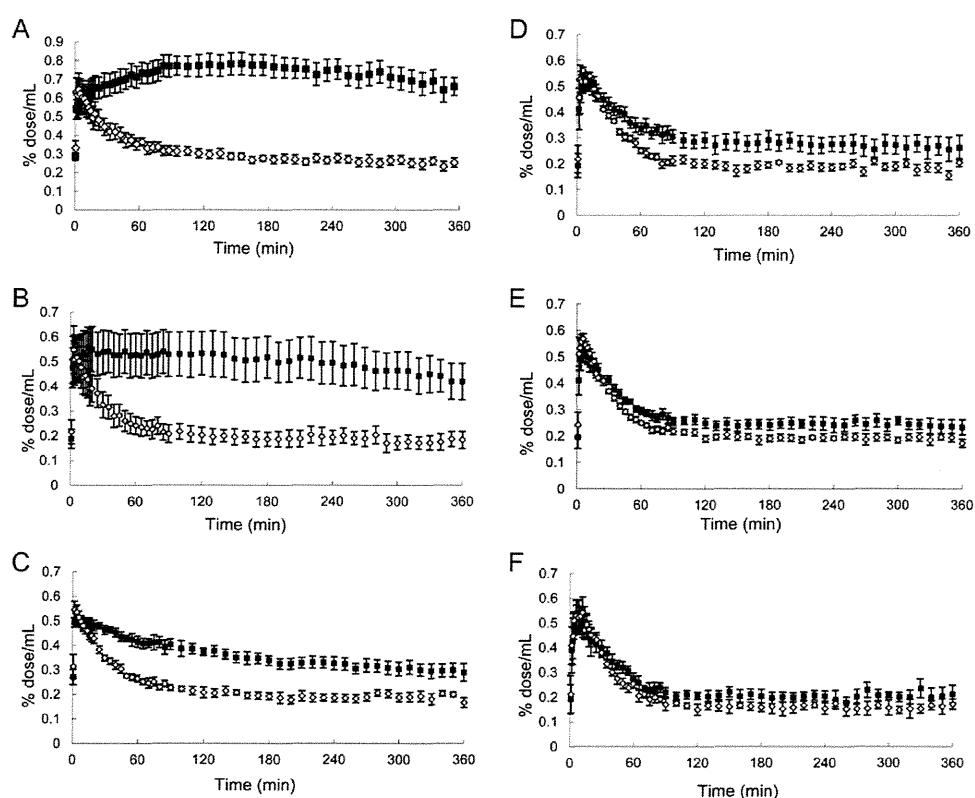
Figure 2. Time–radioactivity curves for [¹⁸F]FE-SPA-RQ in the gerbil striatum (closed squares) and cerebellum (open rhomboids) at baseline (A) and after pretreatments with aprepitant at doses of 0.03 mg/kg (B), 0.1 mg/kg (C), 0.3 mg/kg (D), 3 mg/kg (E), and 30 mg/kg (F). Data were generated by defining ROIs on the PET images displayed in Figure 1. Radioligand uptake into each region was expressed as a percentage of injected dose per unit tissue volume (%dose/mL). Bars indicate standard errors of mean (n = 6 in each treatment group).

Table 1. BP_{ND} of [¹⁸F]FE-SPA-RQ, Striatal NK-1 Receptor Occupancy, and Plasma Aprepitant Concentrations in Gerbils After oral Aprepitant Administration

Parameter	Dose of aprepitant	vehicle (n = 6)	0.03 mg/kg (n = 6)	0.1 mg/kg (n = 5)	0.3 mg/kg (n = 6)	3 mg/kg (n = 6)	30 mg/kg (n = 4)
BP_{ND}		1.70±0.09	1.50±0.18	0.68±0.08	0.44±0.10	0.37±0.08	0.27±0.06
Occupancy (%)		-	11.1±11.1	59.7±5.6	74.9±5.7	78.1±5.1	85.0±2.8
Aprepitant concentration (ng/mL)		-	2.6±0.2	7.4±0.8	26.2±3.5	274.7±10.3	3535.6±707.1

Data are expressed as mean ± standard error of the mean.

outcome measures. In addition, BP_{ND} values calculated by SRTM analysis of dynamic data at 0–120 min were well correlated with those determined with the striatum-to-cerebellum ratio of radioactivity at 120 min (Figure 3C).

Relationship Between Central NK-1 Receptor Occupancy and Plasma Aprepitant Concentration

Concentrations of aprepitant in plasma at the initiation of PET scans were positively correlated with striatal NK-1 receptor occupancy by this drug in gerbils (Figure 4 and Table 1). A direct-model fit to experimental data well described the relationship between receptor occupancy and plasma aprepitant concentration (Figure 4). Maximal receptor occupancy was 85%, and the plasma aprepitant concentrations required for 50%, 90%, and 95% of maximal occupancy (EC_{50}, EC_{90}, and EC_{95}) were 5.5, 50, and 105 ng/mL, respectively.

We noted a large variability of estimates of NK-1 receptor occupancies below 10%, and a slightly excess in the number of data sets around the plateau of the occupancy. However, maximal receptor occupancy and EC_{50} were 85.3% and 3.8 ng/mL, respectively, when data points below the x-axis and beyond 1 000 ng/mL of plasma aprepitant concentration were excluded from the curve fit, and these values were not profoundly different from the original results.

NK-1 Receptor Occupancy by Aprepitant Quantified by Ex Vivo Autoradiography

To examine the validity of in vivo PET measurements of central NK-1 receptor occupancies, brain samples were collected from gerbils at time points ranging from 0.5 to 24 h after treatment with aprepitant at 3 different doses. Then, autoradiography was performed by reacting [¹⁸F]FE-SPA-RQ with coronal sections of

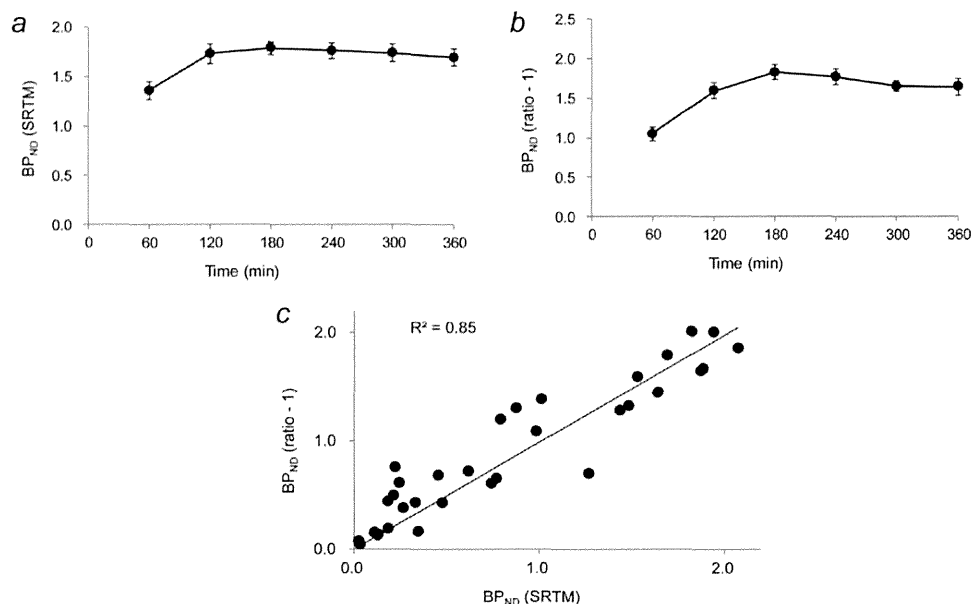Figure 3. PET quantification of radioligand binding in the gerbil striatum. Time stability of [18F]FE-SPA-RQ binding potential values obtained by SRTM (BP_{ND}; A) and on the basis of the target-to-reference ratio of radioactivity (B). Baseline data without pretreatments were used for calculations. In panel B, regional radioactivity was quantified by averaging 15 min dynamic data, and binding potential was determined as (striatum-to-cerebellum ratio) – 1. (C) Scatterplot demonstrating the relationship between BP_{ND} values determined by SRTM analysis of data at 0–120 min and the target-to-reference ratio of radioactivity at 120 (112.5–127.5) min. Parameters were calculated using data at baseline and after pretreatment with aprepitant at doses of 0.03, 0.1, 0.3, 3, and 30 mg/kg. The solid line indicates regression (y = 0.99x).
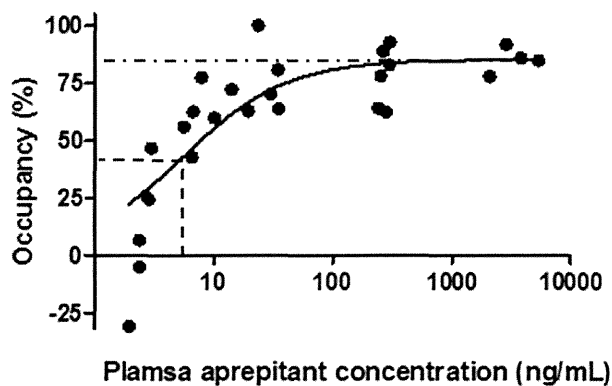

Figure 4. Relationship between plasma aprepitant concentration and NK-1 receptor occupancy by apretitant in the gerbil striatum calculated using [18F] FE-SPA-RQ-PET data. The regression curve was generated using the following equation: receptor occupancy = maximal receptor occupancy × $C_p/[C_p + EC_{50}]$. The dot-dashed line represents the maximal receptor occupancy (85%), and the horizontal and vertical dashed lines denote the half-maximal occupancy (42.5%) and EC_{50} (5.5 ng/mL). respectively.

these brains. Similar to the PET images, autoradiograms demonstrated intense radiolabeling of the striatum, which was completely abolished by the addition of 10 µM aprepitant to the solution (Figure 5A). Based on data from ex vivo autoradiograms after treatment with 0.3 mg/kg aprepitant (top row in Figure 5A), the temporal changes in receptor occupancy (Figure 5B and Table 2) indicated the establishment of an equilibrium between unbound aprepitant plasma and brain compartments within 4 h, justifying the initiation of PET assays at 4 h. In a scatterplot of receptor occupancy by aprepitant and its plasma concentration, data from samples collected 0.5 and 1 h after treatment with 0.3 mg/kg aprepitant could not be described by a direct pharmacokinetic-pharmacodynamic link, presumably due to

incomplete equilibrium between plasma and brain compartments for free drugs at these time points (Figure 5B). By excluding these data from the model fit, EC_{90} and EC_{95} values were estimated to be 16 and 34 ng/mL, respectively.

In Vivo PET of NK-1 Receptor Occupancy in a Marmoset

PET imaging of NK-1 receptors in the marmoset brain was conducted with [18F]FE-SPA-RQ to eliminate the influence of spillover radioactivity from extracranial tissues on the quantification of striatal receptor occupancies. The highest and lowest retention of [18F]FE-SPA-RQ in the brain was observed in the striatum and cerebellum, respectively, as in the gerbil PET analyses (Figure 6A). Unlike the data from gerbils, pretreatment with 20 mg/kg aprepitant decreased striatal radioactivity to a level nearly equivalent to that of the cerebellum, despite increased initial radioligand uptake into all regions (Figure 6A and B). Using radioligand retention at 180 min after injection as a quantitative index, receptor occupancy by aprepitant in the striatum was estimated to be 102.5%, indicating that complete receptor occupancy can be demonstrated by marmoset PET. In the marmoset, a pseudo-equilibrium state of specific radioligand binding was not observed in dynamic PET scans over 180 min, implying that a longer PET measurement would be required to determine pharmacokinetic-pharmacodynamic relationships.

Plasma Protein Binding of Aprepitant

Protein binding of 0.1 µg/mL aprepitant in human and gerbil plasma was measured by ultracentrifugation. Both human and gerbil plasma samples displayed a high degree of protein binding: 99.64% and 99.30%, respectively. Accordingly, unbound aprepitant fractions in human and gerbil plasma were 0.36% and 0.70%, differing by approximately 2 fold.